Desalination and Water Treatment
www.deswater.com
doi: 10.5004/dwt.2019.24325

161 (2019) 343–353
September

Synthesis and application of iron/copper bimetallic nanoparticles doped natural zeolite composite coupled with ultrasound for removal of arsenic (III) from aqueous solutions

Abdolmotaleb Seid-Mohammadi[a], Ghorban Asgari[a], Alireza Rahmani[a], Tayyebeh Madrakian[b], Amir Karami[c,*]

[a]*Social Determinants of Health Research Center, Department of Environmental Health Engineering, School of Public Health, Hamadan University of Medical Sciences, Hamadan, Iran, Tel. +989183729180; email: sidmohammadi@umsha.ac.ir (A. Seid-Mohammadi), Tel. +989123609313; email: asgari@umsha.ac.ir (G. Asgari), Tel. +989181114763; email: rahmani@umsha.ac.ir (A. Rahmani)*

[b]*Faculty of Chemistry, Bu-Ali Sina University, Hamedan, Iran*

[c]*Department of Environmental Health Engineering, School of Public Health, Hamadan University of Medical Sciences, Hamadan, Iran, email: amir_karami119@yahoo.com*

Received 13 October 2018; Accepted 25 April 2019

ABSTRACT

The removal of arsenic (III) from aqueous solutions was investigated using zeolite supported by nano zero-valent iron/copper bimetallic composite (Z-nZVI/Cu) coupled with Ultrasound. The bimetallic nZVI/Cu nanoparticles incorporated into zeolite were prepared using an ion exchange method and were characterized using transmission electron microscopy, X-ray diffraction, Fourier-transform infrared spectroscopy and Brunauer–Emmett–Teller. The results of the analyses showed that ZVI/Cu nanoparticles were successfully distributed on the zeolite. The highest As (III) removal efficiency by ultrasonic process coupled with Z-nZVI/Cu was obtained at pH of 5, As (III) concentration of 1 mg/L, catalyst dosage of 0.3 mg/L, ultrasonic frequency of 80 kHz and reaction time of 60 min. The experiments showed that the As (III) removal efficiency was decreased by increasing the initial pH and As (III) concentration, but it was increased by increasing the catalyst dosage and ultrasonic frequency. The results of the comparative experiments showed that the presence of the ultrasonic process in the solution containing Z-nZVI/Cu is led to increasing the removal of As (III) by dispersing the nanoparticles and increasing the specific surface area, as well as cleaning the catalyst surface and improving the transfer of pollutant mass between bulk solution and catalyst surface. Further study on the treatment of real water sample confirmed the applicability of the ultrasonic system coupled with the catalyst in the removal of As (III). This study showed that the ultrasonic process coupled with Z-nZVI/Cu can be effectively used to remove As (III) from aqueous solutions.

Keywords: Arsenic; Ultrasound; Zeolite; Metallic nanoparticles

1. Introduction

The pollution of aquatic environments by inorganic contaminants is one of the major concerns of the world [1–3]. Arsenic, as a Class A human carcinogen, is an inorganic compound, which is recently known as one of the greatest environmental hazards in the world [4,5]. This pollutant is introduced into the ecosystem through toxic chemicals of agriculture, gold mining, biological activity, geochemical reactions and other anthropogenic activities [6]. Arsenic is

* Corresponding author.

observed in organic and inorganic forms and various oxidation states in aquatic environments depending on pH and Redox conditions. Among them, As (III) is more toxic and more mobile compared to other forms of arsenic [6,7]. Long-term exposure to the water contaminated by As (III) causes the cardiovascular, gastrointestinal, black foot, skin and kidney cancers [7,8]. Therefore, the World Health Organization (WHO) and the Environmental Protection Agency (EPA) reduced their maximum concentration levels from 0.05 to 0.01 mg/L to decline the exposure to arsenic compounds [9]. Conventional methods for removal of arsenic from aqueous environments include adsorption, membrane processes, chemical precipitation, biosorption, coagulation and filtration, ion exchange and chemical oxidation [10–12]. Compared to these technologies, the chemical reduction has recently been considered as a simple and effective technique to eliminate the metals from aqueous solutions. In this process, the metals are converted into the less toxic forms, which can be easily removed by subsequent process, e.g., the adsorption and precipitation processes [13].

In recent years, zero-valent iron nanoparticles (NZVI) have been used as a reducing material in the treatment of harmful organic and inorganic materials [13,14]. In addition, the NZVI due to the small size, high specific surface, non-toxic and low-cost has been considered as a promising substance in environmental engineering for elimination and reduction of the toxicity of pollutants such as chlorine, disinfection by-products, metal ions, chlorinated aliphatic and aromatic compounds [15,16]. However, this method has the disadvantage in treatment processes such as a tendency to accumulate, rapid deposition on a solid surface and application in acidic pH to remove the organic pollutants [16,17]. In addition, the results of previous studies have shown that NZVI is rapidly consumed and it produces large amounts of ferrous and ferric hydroxide [17].

Many attempts have been made to obtain the sustained suspension of NZVI and to reduce its deposition on the surfaces by altering the NZVI surface [16]. One of the methods is the addition of the copper to the NZVI to design the Fe/Cu composite due to faster reaction kinetics, slower deposition of corrosion byproducts on the particle surface and a suitable price of the copper [18,19]. Recently, the use of Fe/Cu bimetallic nanoparticles has found great popularity in various treatment processes. For example, Li et al. [20] synthesized and used the Fe/Cu composite as a Fenton-like catalyst for oxidation of the methylene blue. The results showed that copper metal, by accelerating the Fe^{3+}/Fe^{2+} cycle, provides the rapid decomposition of the H_2O_2 to produce the radical hydroxyl. Xiong et al. [18] reported that Fe/Cu bimetallic had a higher catalytic activity than Fe alone. Hosseini et al. [16], by investigating the reduction of nitrate by Fe/Cu nanoparticles, reported that the bimetallic nanoparticles have the high ability to reduce the nitrate to nitrogen and ammonium gas. However, for a catalyst or effective reducing material, there are still problems such as low availability of active metal sites, metal loss during activity, and reduction in the scattering of the metals [21]. To eliminate these disadvantages, the use of support materials such as activated carbon [22], clay [23], zeolite [24] and carbon nanotube [25] has developed. Among them, zeolite is a favorable substance because of its high specific surface area, high ionic exchange stability, high hydrothermal stability and uniform micropores [21,26]. However, in some studies, it has been reported that the effect of bimetallic nanoparticles on support materials during the process can be reduced by increasing the resistance of the mass transfer by the support material and the decreasing the reaction rate between the contaminants and the nanoparticles [13]. Therefore, a new method is needed to increase the reactivity of nanoparticles and to prevent the accumulation.

The ultrasonic process, as a promising method, has attracted much attention to increasing the mass transfer between the liquid-solid phase and continuous cleaning the surface of metals through the effect of cavitation in the process of oxidation and reduction [27]. In addition, ultrasonic is used as a mixer to reduce the accumulation of nanoparticles and to produce the homogeneous suspensions. Additionally, studies have reported that the presence of ultrasonic with nanoparticles reduces the particle size, eliminates the corrosion products, and produces high amounts of reactive oxygen species [13,28]. However, the application of the ultrasonic process alone needs for a long time and high energy to complete degradation of the organic pollutants. Previous studies reported that this limitation can be eliminated through the application of this process combined with a suitable catalyst; the use of the appropriate catalyst along with the ultrasonic irradiation can lead to increasing the production of more $^{\bullet}OH$ radicals and, consequently, increasing the degradation efficiency [29]. In a study conducted by Hassani et al. [30] for removal of AO7 dye, it was observed that increasing the ultrasonic power has a positive effect on removal of the dye; they reported that increasing the ultrasonic power is led to increasing the mass transfer, production of reactive radicals and generation of further active sites on the catalyst surface which result in improvement of degradation efficiency. In another study, Qiao et al. [31] studied the sonocatalytic degradation of tetracycline using a ternary $SrTiO_3/Ag_2S/CoWO_4$ composite; they also observed that increasing the ultrasonic irradiation power has led to increasing the degradation of tetracycline. Moreover, Cui et al. [32] studied the arsenite oxidation using the Ultrasound/Iron and observed that this method is able to provide significant arsenite removal efficiency (more than 99.1%) by US450 kHz.

Despite the problems associated with As (III) and the excellent properties of Fe/Cu bimetallic and ultrasonic, no study has conducted on the combination of the ultrasonic and Z-nZVI/Cu bimetallic composite for removing the arsenic. Therefore, the purpose of this study was to synthesize the zeolite-supported bimetallic nZVI/Cu (Z-nZVI/Cu) and to evaluate its application with ultrasonic for removing of As (III). The effect of different operational parameters on the As (III) removal was investigated. In addition, the kinetics of the effect of parameters on the removal of As (III) in an ultrasonic system coupled with the Z-nZVI/Cu was studied.

2. Materials and methods

2.1. Materials

Natural zeolite was provided from Sigma Aldrich Company (Germany). All chemicals including ferrous sulfate ($FeSO_4{\cdot}7H_2O$), cupric sulfate ($CuSO_4{\cdot}5H_2O$), sodium

hydrochloride ($NaBH_4$), and sodium hydroxide (NaOH) were purchased from Sigma Aldrich (Germany). Hydrochloric acid (HCl), ethanol and sodium arsenite ($NaASO_2$) were provided from the Merck Company, (German). All chemicals used in this study were of analytical grade and were used without additional purification. Double distilled water was used in each step to prepare suspensions and solutions.

2.2. Synthesis of Z-nZVI/Cu bimetallic nanomposite

Synthesis of zeolite supported nano zero-valent iron/copper bimetallic composite (Z-nZVI/Cu) was performed by ion exchange method. The mesh number of zeolite was surface area: 940–1,000 m^2/g, pore size: 4.6–8 nm and pore volume: 2.5–3 nm. Prior to synthesis, zeolite was sieved through the mesh screen and was immersed in a 20% HCl solution for 24 h and was then washed with distilled water. After removing the impurities, 0.5 g zeolite was added to 300 ml of a solution containing 0.025 gr $CuSO_4{\cdot}5H_2O$ and 1 gr $FeSO_4{\cdot}7H_2O$. The pH of the solution was adjusted to 4 by using HCl to prevent the effect on the zeolite stability, as well as the oxidation of iron and copper. The resultant mixture was kept for 30 min under ultrasonic conditions and then mixed for 30 min. The mixture was then filtered using a 45 μm filter and the remaining solid was transferred to a three neck flask containing 50 ml of deoxygenated water. Under nitrogen gas, a $NaBH_4$ (1 M) solution was added dropwise to a continuous flask. After formation of a black solution, the Z-nZVI/Cu composite was separated using the filter, was washed with distilled water and ethanol and was then dried under vacuum at 60°C for 24 h. Bimetallic nanoparticles nZVI/Cu were prepared under the same conditions without the addition of zeolite [28].

2.3. Characterization of Z-nZVI/Cu bimetallic composite

The morphology and the elements of Z-nZVI/Cu were determined by a scanning electron microscope (SEM) coupled with energy dispersive X-ray spectroscopy (EDX) (Dazheng PS-305D, China). Transmission electron microscopy (TEM, JEOL model, USA) was used to determine the size and distribution of nZVI/Cu bimetallic on the zeolite surface. The Z-nZVI/Cu structure was studied using the X-ray diffraction (XRD, Bruker, Germany) with Cu Ka radiation in 40 kV and 40 mA by scanning in the range of 10°–80°. Nitrogen adsorption-desorption isotherms were obtained using the Brunauer–Emmett–Teller (BET) method (Micromeritics, USA) and were used to find pore size, volume size and specific surface area of the prepared catalyst. Evaluation of functional groups on the surface of the Z-nZVI/Cu in the range of 4,000–400 cm^{-1} was performed by Fourier-Transform infrared spectroscopy (FTIR, Bruker, Germany).

2.4. Experimental method

As (III) removal was carried out in a 250 ml conical flask placed in an ultrasonic bath containing a constant frequency of 80 kHz and at a temperature of 30°C (Fig. 1). To determine the As (III) removal efficiency, the experiments were carried out at various initial pH values (5–8), Z-nZVI/Cu dosage (0.1–0.4 mg/L), As (III) concentration (1–5 mg/L) and ultrasonic frequency (37 and 80 kHz). The impact of factors was tested by changing a parameter and keeping constant other factors. Samples were taken at appropriate time intervals from the reaction vessel with a 10 mL syringe and filtered through 0.45 μm membranes for separating the Z-nZVI/Cu. The residual As (III) concentration was then measured by inductively coupled plasma optical emission spectroscopy (ICP-OES) (PQ9000/Elite-Germany). In the process of experiments, the pH of the solution was kept constant by phosphate buffer and adjusted by 0.01 HCl or NaOH. To evaluate the efficiency of the Z-nZVI/Cu-coupled ultrasonic process, a real water sample prepared from Bijar city of Iran was used. The removal efficiency (RE) of As (III) and pseudo-first order kinetic was calculated using Eqs. (1) and (2).

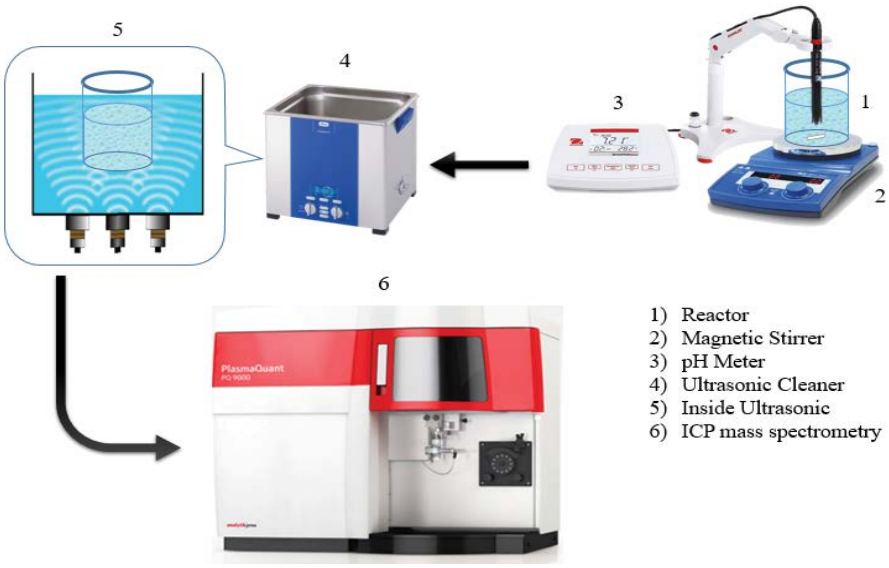

Fig. 1. Schematic of the process studied.

$$\mathrm{RE}(\%) = \frac{C_0 - C_e}{C_0} \times 100 \quad (1)$$

$$\mathrm{Ln}\left(\frac{C_0}{C_e}\right) = Kt \quad (2)$$

where K is the first-order rate constant, t is the reaction time, C_0 and C_e are the initial and final concentrations of As(III), respectively.

Experiments were carried out at room temperature to prevent the temperature rise in the reactor circulating operation during the test.

2.5. Validation and verification methods were performed as follows

- We made synthetic concentrations of pollutants during the tests and measured them by the ICP-OES machine which showed the proper functioning of the device to measure the concentration of the contaminant.
- *Calculation of limit of detection (LOD) and limit of quantification (LOQ):* First, we prepared a Blank and injected it into the machine and repeated it at least 5 times and we obtained a standard deviation (S_b) for Blank.

  LOD: (3 × standard deviation)/slope of the line equation

  LOQ: (10 × standard deviation)/slope of the line equation

  Calibration data: R^2 = 0.999321790, m = 69,028,192 and S_b = 0.0089094 mg/L

  BEC: $Y = a + bx$; a = 15.130501 and b = 6,902.8192

2.6. Optimization of process

In order to optimize the studied parameter, the experiments were carried out by varying one of the parameters and keeping constant other parameters. The value of non-constant parameter in which the highest removal efficiency was obtained was selected as the optimum value.

3. Results and discussion

3.1. Characterization of Z-nZVI/Cu bimetallic composite

The morphology and structure of zeolite and Z-nZVI/Cu obtained by SEM and TEM images are shown in Fig. 2. As shown in Figs. 2a and b, the zeolite has a smooth surface, while the Z-nZVI/Cu bimetallic composite has the polygonal and abrasive structure. The TEM image (Fig. 2c) showed that the nZVI/Cu is distributed in the form of black spots on the entire zeolite surface. The EDX analysis, represented in Fig. 3, was performed to determine the elements and revealed that natural zeolite has no iron and copper metal content, while the Z-nZVI/Cu has high iron and copper concentrations.

The XRD pattern of nZVI/Cu and Z-nZVI/Cu is shown in Fig. 4. The XRD profile in Fig. 4a clearly shows the presence of copper with diffraction peaks at 43.32° and 53°. The diffraction peaks at 47.12° and 67.99° are related to α-Fe^0, which confirms the presence of zero-valent iron in the Fe/Cu bimetallic composite. In addition, the XRD pattern of nZVI/Cu exhibits the presence of Fe_2O_3 at 27.37°, while the sharp peak at 38.26° may be related to $CuFeO_2$. In Fig. 4b, the zeolite diffraction peak is not detected, which indicates the strong interaction of iron and copper nanoparticles with zeolite and the crystalline growth of metals between the zeolite layers.

The textural properties of the Z-nZVI/Cu are shown in Table 1. As seen, filling nitrogen occurs approximately at P/P_0 = 0.99, which indicates a high degree of pore size of the catalyst. The BET specific surface of Z-nZVI/Cu is 174.64 m^2/g, which is much higher compared with the zeolite specific surface reported by Danish et al. [33]. This could be related to the incorporation of iron and copper nanoparticles into zeolite. The average pore size and the pore volume of Z-nZVI/Cu were 8.05 nm and 0.35 cm^3/g, respectively, which are well agreed with Danish et al. [34]. The FTIR spectrum of zeolite and Z-nZVI/Cu obtained in the range of 4,000–400 cm^{-1} is shown in Fig. 5. According to this figure, the characteristic peaks at 3,450 and 1,635 cm^{-1} are related to the stretching vibration of OH [26] and the band near 465, 680 and 1,100 cm^{-1} are related to stretching and bending vibration of Al–O–Si in zeolite [34]. The changed spectral peaks in 440 and 535 cm^{-1} show the presence of cations such as iron nanoparticles [33], while the stretching peak near

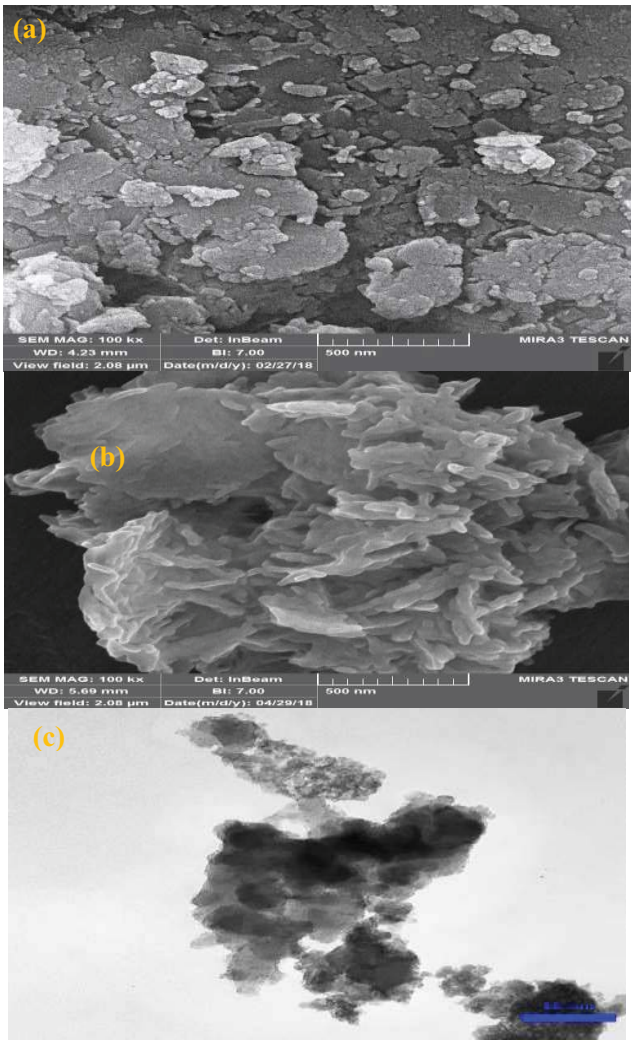

Fig. 2. SEM micrograph of (a) zeolite, (b) Z-nZVI/Cu, and (c) TEM micrograph of Z-nZVI/Cu.

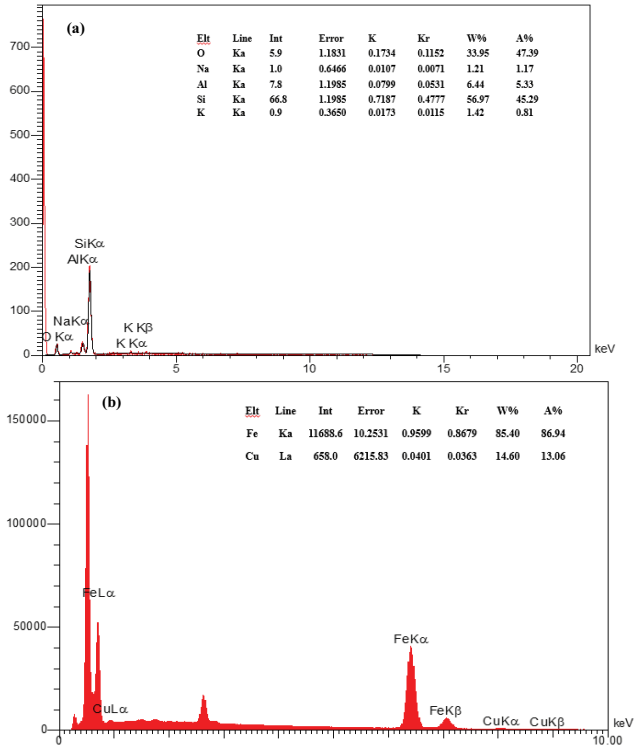

Fig. 3. EDX of (a) zeolite and (b) Z-nZVI/Cu.

Table 1
Textural characterization of Z-nZVI/Cu

Pore volume (cm^3/g)	0.35
Pore size (nm)	8.05
BET surface area (m^2/g)	174.64
P/P_0	0.99

990 cm^{-1} is due to the presence of copper on the Al–O–Si Bridge [34]. In addition, the appearance of new spectral peaks and the changes in the intensity of other peaks in the FTIR of the Z-nZVI/Cu shows the interaction of iron and copper nanoparticles with zeolite [33].

3.2. As (III) removal in various systems

Fig. 6 shows the As (III) removal efficiency in different systems at pH of 5 and ultrasonic frequency of 37 kHz. According to this Fig, the removal of As (III) by ultrasonic at different reaction times is between 4%–18%. This low efficiency is due to the production of low amounts of oxidants during water decomposition. The correction coefficient (R^2) for pseudo-first-order kinetic model was >0.93. These results are consistent with Wang et al. [27]. The results of Fig. 6 also show that the As (III) removal efficiency by the ultrasonic and Z-nZVI/Cu at the various reaction times is 6%–11% greater than that of the Z-nZVI/Cu alone. These results were

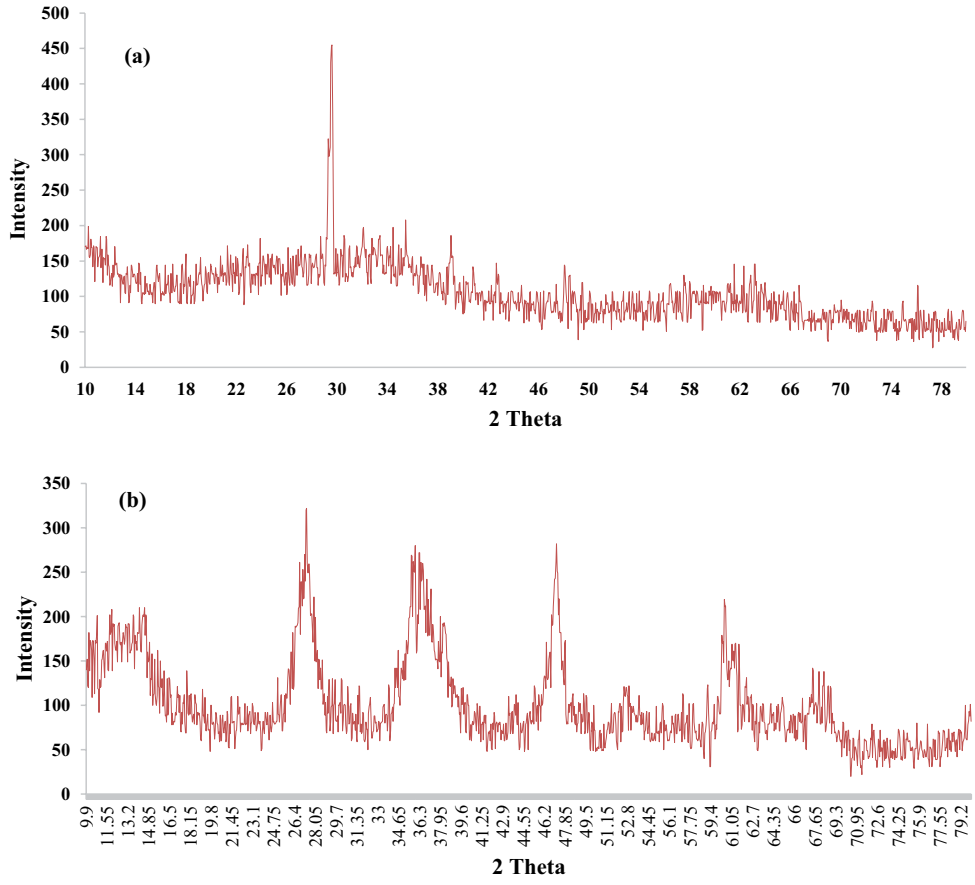

Fig. 4. XRD pattern of (a) Z-nZVI/Cu and (b) nZVI/Cu metallic nanoparticles.

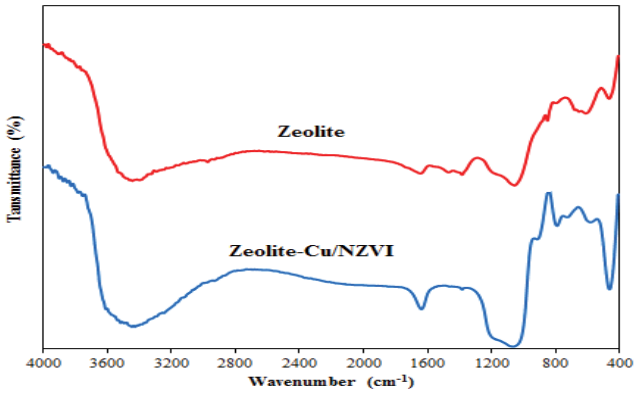

Fig. 5. FTIR spectrum of zeolite and Z-nZVI/Cu.

confirmed by the constant reaction rate shown in Fig. 6b. This can be explained by the fact that the application of ultrasonic in the process containing the catalyst and pollutant is led to accelerating the mass transfer rate of As (III) into Z-nZVI/Cu. Then, the metals hydroxides are formed through the reaction between the As (III) and metals of nZVI/Cu bimetallic. At the same time, by reduction of Fe^0 to Fe^{2+}, the As (III) is converted into As (V). In addition, at the presence of ultrasonic in the reaction solution, the dispersion, cleaning, and activation of the catalyst occur, which result in the reduction or elimination of As (III) [13,35]. Zhou et al. reported that, by combining the ultrasonic process with nZVI, the removal efficiency of chromium is increased by accelerating the mass transfer and increasing the chromium reaction with the nanoparticle surface [13]. Sun et al. [17] investigated the removal of nitrobenzene by Fe/Cu bimetallic catalyst and reported that bimetallic catalyst by the production of iron hydroxide and radical hydroxyl is led to eliminating the nitrobenzene through adsorption, precipitation and oxidation processes. In this study, the results also showed that nitrobenzene can be converted into aniline during the reduction process of Fe to Fe^{2+}.

3.3. Effect of initial pH

The pH of the solution is one of the important parameters for the removal of organic and inorganic contaminants due to the control of the metals concentration in the catalyst and the production rate of various oxidants [31]. The effect of different pH on the As(III) removal efficiency was investigated under the initial concentration of As(III) of 1 mg/L, temperature of 30°C, frequency of 80 kHz and catalyst dosage of 0.025 mg/L and the results are shown in Fig. 7. It can be seen that, by increasing the pH from 5 to 8, the As (III) removal efficiency is reduced.

The kinetic constant rate was decreased from 0.0236 to 0.015 min^{-1} when the initial pH increased from 5 to 8. The correlation coefficient (R^2) for pseudo-first-order kinetic model was >0.75.

These observations of the results can be explained by the effect of pH on the Z-nZVI/Cu and ultrasonic reaction [28,36]. In the acidic condition, high levels of hydrogen ions are led to increasing the corrosion rate of the Z-nZVI/Cu and to increasing the production and reactivity of Fe^{2+} in the presence of ultrasonic [13,27]. The presence of both hydrogen and Fe^{2+} ions reduces the As (III) to As (V) [13,37]. Compared to this situation, in alkaline pH, the accessibility of the As (III) to Z-nZVI/Cu surface is reduced by formation of the metal hydroxide and, subsequently, reduction of the reactive site of the catalyst [38]. Similar results were reported by He et al. to remove nitrate and phosphate by Z-Fe/Ni bimetallic nanoparticles [26].

In addition to the above considerations, the changes in the As (III) removal efficiency at pH values in the range 5–8 can be attributed to the ionization properties of Z-nZVI/Cu and

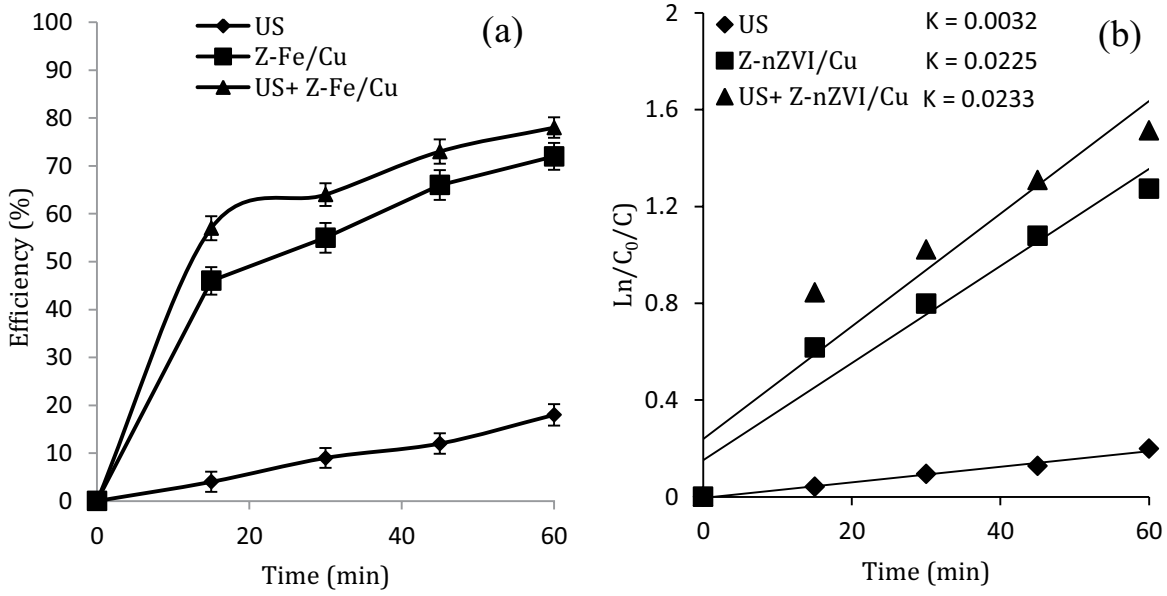

Fig. 6. Changes of As (III) removal efficiency (a) kinetic constant and (b) by Us, Z-nvi/Cu and Us-Z-nzvi/Cu at temperature = 30°C, pH = 5, adsorbent dose = 0.3 g/L, contact time = 60 min, As (III) concentration = 1 mg/L and frequency 80 kHz.

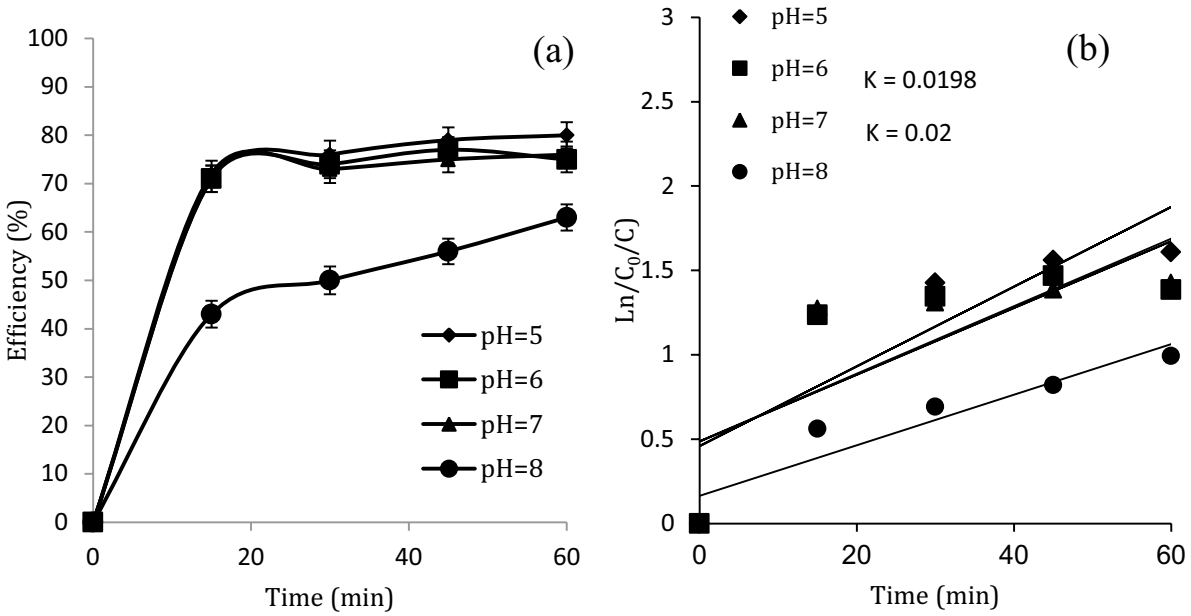

Fig. 7. Effect of changes pH on As (III) removal efficiency (a) kinetic constant and (b) by Us-Z-nzvi/Cu at temperature = 30°C, pH = 5, adsorbent dose = 0.3 g/L, contact time = 60 min, As (III) concentration = 1 mg/L and frequency = 80 kHz.

As (III). The ionization state of the Z-nZVI/Cu surface and As (III) at different pH values depends on the point of zero charge (PZc). According to Babaee et al. [39], the PZc of Fe/Cu nanoparticles is between 8 and 9, which means that the surface charge of the nanoparticles was positive at the pH values lower than PZc and was negative at the values higher than the mentioned limit. Simultaneously, at the pH values below 9, the As (III) is mainly in form of neutral H_3ASO_3, while its dominant form, at pH higher than 9, is $H_2ASO_3^-$. Moreover, the dominant form of arsenate in the pH range from 5 to 11 is $HASO_4^{2-}$. Considering these cases, within the studied pH range, there is the potential for adsorption of As (III) and its reduced form (arsenate), as well as the possibility for catalytic activity of Z-nZVI/Cu in removing the contaminants.

3.4. Effect of Z-nZVI/Cu dosage

Effect of different dosages of Z-nZVI/Cu (0.05–0.4 mg/L) on As (III) removal efficiency was evaluated under the conditions, i.e., pH of 5, initial concentration of 1 mg/L As (III), temperature of 30°C, frequency of 80 kHz. The results obtained in Fig. 8 showed that the As (III) removal efficiency significantly increased from 0.05 to 0.3 mg/L by increasing the Z-nZVI/Cu dosage. However, by the further increase in Z-nZVI/Cu dosage, no significant effect was observed in the As (III) removal. For example, removal of As (III) at 30 min was increased from 76% to 79%, 82% and 84% when catalyst dosages were 0.05, 0.1, 0.2 and 0.3 mg/L. However, no significant differences were observed for the catalyst dosages of 0.3 and 0.4 mg/L. Therefore, the dosage of 0.3 mg/L was chosen as the optimum dosage of Z-nZVI/Cu for the next experiments. The results of the first-order kinetic constant showed the same trend (Fig. 7b). The correlation coefficient (R^2) for the pseudo-first-order kinetic model was >0.95. Increasing the As (III) removal efficiency by more loading of Z-nZVI/Cu may be associated with an increase in active sites available for chemical reactions and adsorption. Similar results were observed by Danish et al. for the degradation of trichloroethylene using the zeolite containing nZVI/Cu nanoparticles [34]. Mosaferi et al. [4] reported that increasing the dosage of nZVI on starch and carboxymethylcellulose is led to develop the As (III) removal efficiency. Asfaram et al. [40] investigated the effect of ultrasound coupled with activated carbon containing the Mn–Fe_3O_4 nanoparticles and found that the cationic dyes removal efficiency increases by increasing the carbon/Mn–Fe_3O_4 composite, due to increasing the active sites for the adsorption process and chemical reactions.

3.5. Effect of ultrasonic frequency

The effect of ultrasonic frequencies of 37 and 80 kHz on As (III) removal efficiency was studied at pH of 5, initial concentration of 1 mg/L As (III), temperature of 30°C and catalyst dosage of 0.3 mg/L. Fig. 9a shows that, by increasing the ultrasonic frequency, the As (III) removal efficiency was increased from 78% to 89%. The results of kinetic analysis also showed that the As (III) removal rate increases with increasing the frequency (Fig. 9b). The correlation coefficient (R^2) for pseudo-first-order kinetic model was >0.89. This can be due to increasing the turbulence of the solution and increasing the mass transfer rate of As (III), intermediates and oxidants between the bulk solution and the catalyst surface. In addition, increasing the frequency is led to increasing the effect of the wave on the dispersing and increasing the specific surface of the catalyst. It is also resulted in cleaning and removing the by-product from the catalyst surface. Increasing the As (III) removal can also be attributed to the acceleration of reactions 3 and 4 due to the increase of ultrasonic frequency [13,37]. Similar results were reported by Khataee et al. [41] in the sono-catalytic

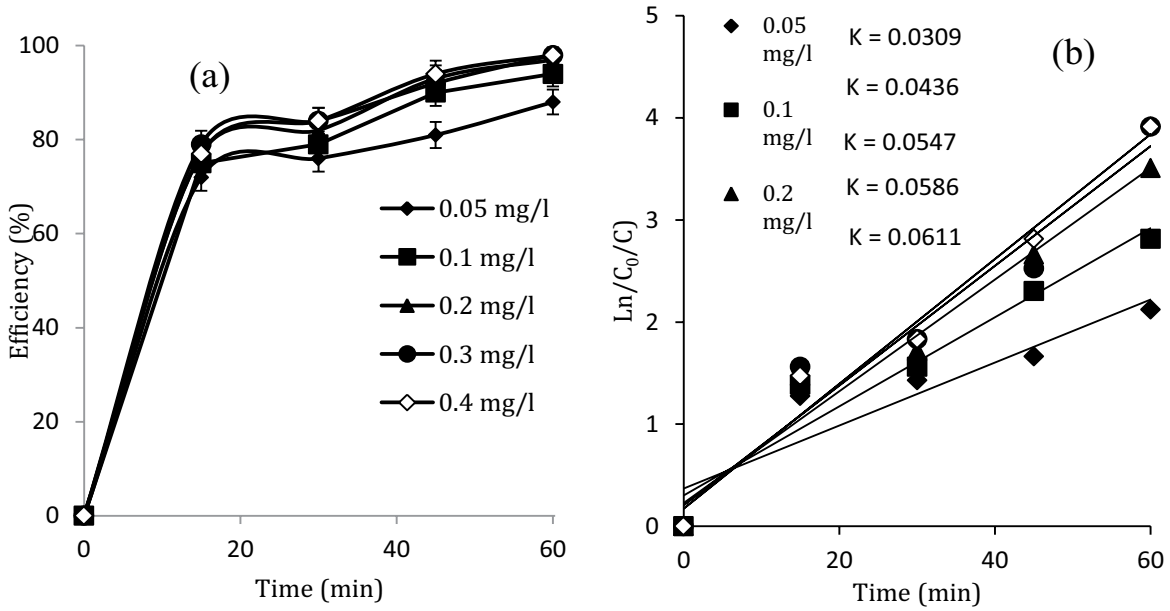

Fig. 8. Effect of changes Z-nzvi/Cu adsorbent dose on As (III) removal efficiency (a) kinetic constant and (b) at temperature = 30°C, pH = 5, As (III) concentration = 1 mg/L, contact time = 60 min and frequency = 80 kHz.

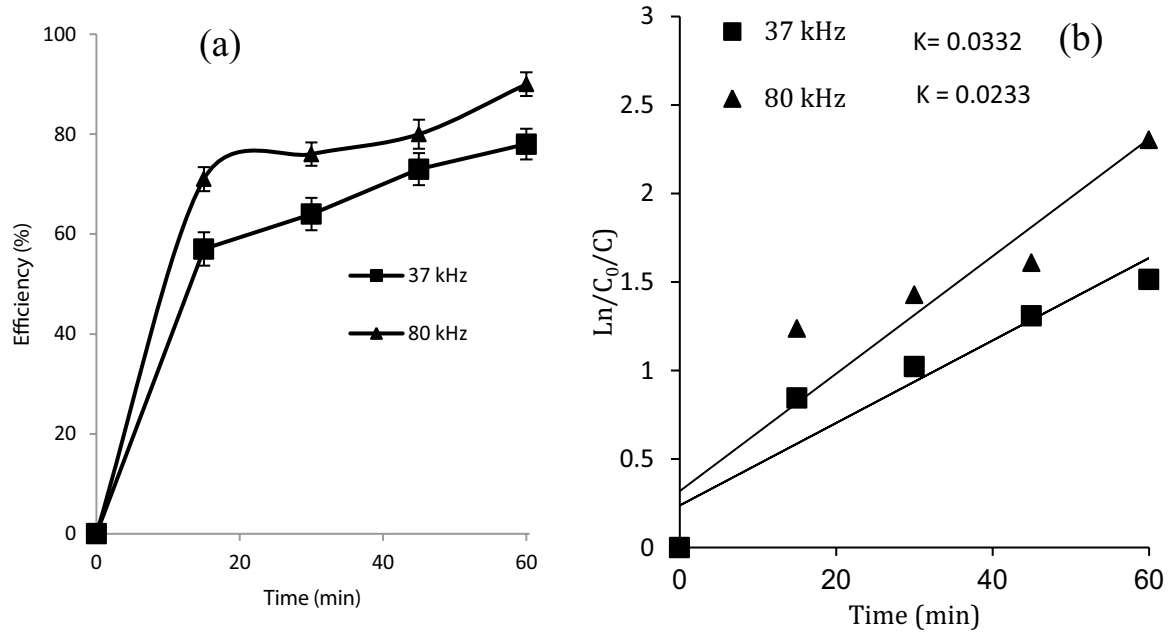

Fig. 9. Effect of changes ultrasonic frequency on As (III) removal efficiency (a) kinetic constant and (b) at temperature = 30°C, pH = 5, As (III) concentration = 1 mg/L, adsorbent dose = 0.3 g/L and contact time = 60 min.

degradation of the acid blue 92 dye. Zhang et al. [42], by studying the effect of the catalyst assisted by ultrasonic on the treatment of the water, reported that the presence of ultrasonic is led to cleaning the products of degradation of pollutants from the catalyst surface.

$$\text{Pollutant} + Fe^{0} + H^{+} \rightarrow Fe^{2+} + \text{product of reduction or degradation} + H_2O \quad (3)$$

$$\text{Pollutant} + Fe^{2+} + H^{+} \rightarrow Fe^{3+} + \text{product of reduction or degradation} + H_2O \quad (4)$$

3.6. Effect of As (III) concentration

The effect of initial concentration of As (III) was studied by changing its concentration from 1 to 5 mg/L at pH of 5, ultrasonic frequency of 80 kHz, temperature of 30°C, and

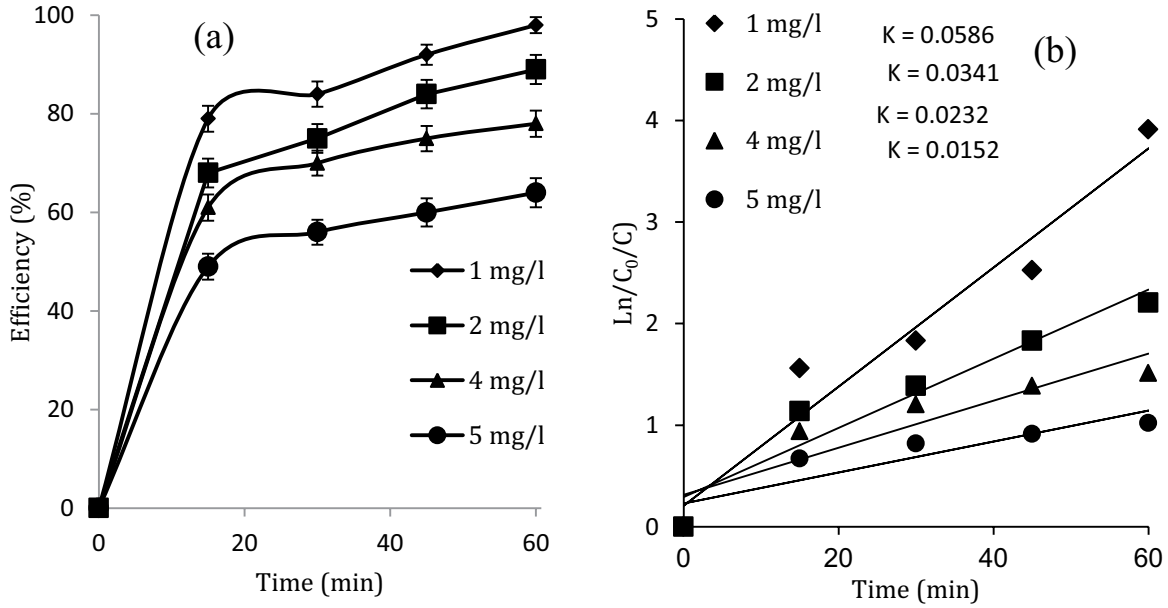

Fig. 10. Effect of changes As (III) concentration on As (III) removal efficiency (a) kinetic constant and (b) at temperature = 30°C, pH = 5, adsorbent dose = 0.3 g/L, contact time = 60 min and frequency = 80 kHz.

catalyst dosage of 0.3 mg/L. The results of Fig. 10a show that, by increasing the As (III) initial concentration, the efficiency of As (III) removal was decreased from 98% to 64% at 60 min. The kinetics analysis results showed the same trend in the efficiency of As (III) removal (Fig. 10b). The correction coefficient (R^2) for the pseudo-first-order kinetic model was >0.91. This can be due to the limitation of active sites of Z-nZVI/Cu for high concentrations of As (III). Similar results were obtained in the studies conducted to remove acid orange 7 [28,35] and chromium metal using the catalyst coupled with ultrasonic [13].

3.7. Treatment of the real water sample

To investigate the applicability of the Z-nZVI/Cu coupled with the ultrasonic process for treatment of the water containing the As(III), the experiments were carried out at pH of 5, ultrasonic frequency of 80 kHz, temperature of 30°C, and catalyst dosage of 0.3 mg/L. The results of Table 2 show that the average removal of nitrate and As (III) in the actual sample using the Z-nZVI/Cu coupled with the ultrasonic process was 87% and 90%, respectively.

Table 2
Characteristics of the groundwater before and after the treatment process

Parameters	Input concentration (mg/L)	Output concentration (mg/L)
Nitrate	68.9	9
As (III)	0.026	0.0026
Iron	0.0137	0.054
Copper	0.0094	0.012

4. Conclusion

In this study, the Z-nZVI/Cu was synthesized and used as a catalyst in the ultrasonic process to increase the removal of As (III) from aqueous solutions. SEM, TEM, EDX, and FTIR analyses showed that nZVI and Cu nanoparticles were successfully coated on the zeolite surface. The nitrogen adsorption-desorption analysis confirmed the high specific surface, suitable pore size and pore volume of the catalyst. The As (III) removal efficiency was increased by increasing the Z-nZVI/Cu dosage and ultrasonic frequency, but it was decreased by increasing the initial pH and As (III) concentration. Comparative experiments showed that the combined ultrasonic and catalyst process has a higher efficiency compared to the ultrasonic and composite process alone. This increase in efficiency can be due to the interaction effects of ultrasonic and catalyst in increasing the chemical reactions and adsorption. The results of the application of the optimum parameters obtained for the actual sample containing As (III) showed that the Z-nZVI/Cu-coupled with the ultrasonic process is capable to provide As (III) removal efficiency of 90%. The results showed that the ultrasonic process combined with Z-nZVI/Cu composite can be used as a promising method for treating the solutions containing toxic metals, especially As (III).

Acknowledgments

This study has been adapted from a PhD student thesis at Hamadan University of Medical Sciences. The study was funded by Vice-Chancellor for Research and Technology, Hamadan University of Medical Sciences (No. 960928042).

References

[1] P. Sepúlveda, M.A. Rubio, S.E. Baltazar, J. Rojas-Nunez, J.S. Llamazares, A.G. Garcia, N. Arancibia-Miranda, As(V)

removal capacity of FeCu bimetallic nanoparticles in aqueous solutions: the influence of Cu content and morphologic changes in bimetallic nanoparticles, J. Colloid Interface Sci., 524 (2018) 177–187.
[2] M. Farrokhi, M. Naimi-Joubani, A. Dargahi, M. Poursadeghiyan, H.A. Jamali, Investigating activated sludge microbial population efficiency in heavy metals removal from compost leachate, Pol. J. Environ. Stud., 5 (2018) 6.
[3] A. Almasi, A. Dargahi, M.M.H. Ahagh, H. Janjani, M. Mohammadi, L. Tabandeh, Efficiency of a constructed wetland in controlling organic pollutants, nitrogen, and heavy metals from sewage, J. Chem. Pharm. Sci., 9 (2016) 2924–2928.
[4] M. Mosaferi, S. Nemati, A. Khataee, S. Nasseri, A.A. Hashemi, Removal of arsenic (III, V) from aqueous solution by nanoscale zero-valent iron stabilized with starch and carboxymethyl cellulose, J. Environ. Health Sci., 12 (2014) 74.
[5] K. Taleb, J. Markovski, Z. Veličković, J. Rusmirović, M. Rančić, V. Pavlović, A. Marinković, Arsenic removal by magnetite-loaded amino modified nano/microcellulose adsorbents: effect of functionalization and media size, Arabian J. Chem., (2016), doi.org/10.1016/j.arabjc.2016.08.006 (In Press).
[6] S. Mandal, M.K. Sahu, R.K. Patel, Adsorption studies of arsenic(III) removal from water by zirconium polyacrylamide hybrid material (ZrPACM-43), Water Resour. Ind., 4 (2013) 51–67.
[7] S. Bibi, A. Farooqi, K. Hussain, N. Haider, Evaluation of industrial based adsorbents for simultaneous removal of arsenic and fluoride from drinking water, J. Cleaner Prod., 87 (2015) 882–896.
[8] M. Rahim, M.R.H.M. Haris, Application of biopolymer composites in arsenic removal from aqueous medium: a review, J. Radiat. Res. Appl. Sci., 8 (2015) 255–263.
[9] N. Jaafarzadeh, N. Mengelizadeh, A. Takdastan, M. Haji-Amadi, Kinetic studies on bioadsorption of arsenate from aqueous solutions using chitosan, J. Adv. Environ. Health. Res., 2 (2014) 7–12.
[10] D. Mohanty, Conventional as well as emerging arsenic removal technologies—a critical review, Water Air Soil Pollut., 228 (2017) 381.
[11] K.P. Kowalski, Advanced Arsenic Removal Technologies Review, E.G. Søgaard Ed., Chemistry of Advanced Environmental Purification Processes of Water, Elsevier, 2014, pp. 285–337.
[12] A. Dargahi, H. Golestanifar, P. Darvishi, A. Karami, S.H. Hasan, A. Poormohammadi, A. Behzadnia, An investigation and comparison of removing heavy metals (lead and chromium) from aqueous solutions using magnesium oxide nanoparticles, Pol. J. Environ. Stud., 25 (2016) 557–562.
[13] X. Zhou, B. Lv, Z. Zhou, W. Li, G. Jing, Evaluation of highly active nanoscale zero-valent iron coupled with ultrasound for chromium(VI) removal, Chem. Eng. J., 281 (2015) 155–163.
[14] R.A. Crane, T.B. Scott, Nanoscale zero-valent iron: future prospects for an emerging water treatment technology, J. Hazard. Mater., 211 (2012) 112–125.
[15] P.C. Chiu, Applications of Sero-Valent Iron (ZVI) and Nanoscale ZVI to Municipal and Decentralized Drinking Water Systems—A Review, S. Ahuja, K. Hristovski, Eds., Novel Solutions to Water Pollution, 2013, pp. 237–249.
[16] S.M. Hosseini, B. Ataie-Ashtiani, M. Kholghi, Nitrate reduction by nano-Fe/Cu particles in packed column, Desalination, 276 (2011) 214–221.
[17] L. Sun, H. Song, Q. Li, A. Li, Fe/Cu bimetallic catalysis for reductive degradation of nitrobenzene under oxic conditions, Chem. Eng. J., 283 (2016) 366–374.
[18] Z. Xiong, B. Lai, P. Yang, Y. Zhou, J. Wang, S. Fang, Comparative study on the reactivity of Fe/Cu bimetallic particles and zero valent iron (ZVI) under different conditions of N_2, air or without aeration, J. Hazard. Mater., 297 (2015) 261–268.
[19] Y. Yuan, B. Lai, Y. Tang, P. Yang, Y. Zhou, Comparative study of ammunition wastewater pretreatment by Fe/Cu/Air and Fe^0/air processes, Environ. Eng. Sci., 34 (2017) 197–206.
[20] K. Li, Y. Zhao, M.J. Janik, C. Song, X. Guo, Facile preparation of magnetic mesoporous Fe_3O_4/C/Cu composites as high performance Fenton-like catalysts, Appl. Surf. Sci., 396 (2017) 1383–1392.
[21] C. Dai, A. Zhang, L. Luo, X. Zhang, M. Liu, J. Wang, X. Guo, C. Song, Hollow zeolite-encapsulated Fe-Cu bimetallic catalysts for phenol degradation, Catal. Today, 297 (2017) 335–343.
[22] N. Ping, Y. Lili, Y. Honghong, T. Xiaolong, L. Hua, W. Hongyan, Y. Lina, Effect of Fe/Cu/Ce loading on the coal-based activated carbons for hydrolysis of carbonyl sulfide, J. Rare Earths, 28 (2010) 205–210.
[23] M.N. Timofeeva, S.Ts. Khankhasaeva, E.P. Talsi, V.N. Panchenko, A.V. Golovin, E.T. Dashinamzhilova, S.V. Tsybulya, The effect of Fe/Cu ratio in the synthesis of mixed Fe, Cu, Al-clays used as catalysts in phenol peroxide oxidation, Appl. Catal., B, 90 (2009) 618–627.
[24] B. Fan, H. Li, W. Fan, C. Jin, R. Li, Oxidation of cyclohexane over iron and copper salen complexes simultaneously encapsulated in zeolite Y, Appl. Catal., A, 340 (2008) 67–75.
[25] S. Rezaee, A. Ghaderi, A. Boochani, S. Solaymani, Synthesis of multiwalled carbon nanotubes on Cu-Fe nano-catalyst substrate, Results Phys., 7 (2017) 3640–3644.
[26] Y. He, H. Lin, Y. Dong, B. Li, L. Wang, S. Chu, M. Luo, J. Liu, Zeolite supported Fe/Ni bimetallic nanoparticles for simultaneous removal of nitrate and phosphate: synergistic effect and mechanism, Chem. Eng. Sci., 347 (2018) 669–681.
[27] X. Wang, L. Wang, J. Li, J. Qiu, C. Cai, H. Zhang, Degradation of Acid Orange 7 by persulfate activated with zero valent iron in the presence of ultrasonic irradiation, Sep. Purif. Technol., 122 (2014) 41–46.
[28] A. Wang, W. Guo, F. Hao, X. Yue, Y. Leng, Degradation of Acid Orange 7 in aqueous solution by zero-valent aluminum under ultrasonic irradiation, Ultrason. Sonochem., 21 (2014) 572–575.
[29] A. Hassani, P. Eghbali, Ö. Metin, Sonocatalytic removal of methylene blue from water solution by cobalt ferrite/mesoporous graphitic carbon nitride ($CoFe_2O_4$/mpg-C_3N_4) nanocomposites: response surface methodology approach, Environ. Sci. Pollut., 25 (2018) 32140–32155.
[30] A. Hassani, G. Çelikdağ, P. Eghbali, M. Sevim, S. Karaca, Ö. Metin, Heterogeneous sono-Fenton-like process using magnetic cobalt ferrite-reduced graphene oxide ($CoFe_2O_4$-rGO) nanocomposite for the removal of organic dyes from aqueous solution, Ultrason. Sonochem., 40 (2018) 841–852.
[31] J. Qiao, H. Zhang, G. Li, S. Li, Z. Qu, M. Zhang, J. Wang, Y. Song, Fabrication of a novel Z-scheme $SrTiO_3$/Ag_2S/$CoWO_4$ composite and its application in sonocatalytic degradation of tetracyclines, Sep. Purif. Technol., 211 (2019) 843–856.
[32] M. Cui, M. Jang, S. Lee, B. Kweon, S.-T. Yun, J. Khim, Arsenite oxidation and treatment by ultrasound/iron in aqueous solutions, Jpn. J. Appl. Phys., 50 (2011) 07HE08.
[33] M. Danish, X. Gu, S. Lu, M.L. Brusseau, A. Ahmad, M. Naqvi, U. Farooq, W.Q. Zaman, X. Fu, Z. Miao, An efficient catalytic degradation of trichloroethene in a percarbonate system catalyzed by ultra-fine heterogeneous zeolite supported zero valent iron-nickel bimetallic composite, Appl. Catal., A, 531 (2017) 177–186.
[34] M. Danish, X. Gu, S. Lu, A. Ahmad, M. Naqvi, U. Farooq, X. Zhang, X. Fu, Z. Miao, Y. Xue, Efficient transformation of trichloroethylene activated through sodium percarbonate using heterogeneous zeolite supported nano zero valent iron-copper bimetallic composite, Chem. Eng. Sci., 308 (2017) 396–407.
[35] H. Zhang, L. Duan, Y. Zhang, F. Wu, The use of ultrasound to enhance the decolorization of the C.I. Acid Orange 7 by zero-valent iron, Dyes Pigm., 65 (2005) 39–43.
[36] B. Chen, X. Wang, C. Wang, W. Jiang, S. Li, Degradation of azo dye direct sky blue 5B by sonication combined with zero-valent iron, Ultrason. Sonochem., 18 (2011) 1091–1096.
[37] F. Liang, J. Fan, Y. Guo, M. Fan, J. Wang, H. Yang, Reduction of nitrite by ultrasound-dispersed nanoscale zero-valent iron particles, Ind. Eng. Chem. Res., 47 (2008) 8550–8554.
[38] S. Karthikeyeni, T. Siva Vijayakumar, S. Vasanth, A. Ganesh, V. Vignesh, J. Akalya, R. Thirumurugan, P. Subramanian, Decolourisation of Direct Orange S dye by ultra sonication using iron oxide nanoparticles, J. Exp. Nanosci., 10 (2015) 199–208.

[39] Y. Babaee, C.N. Mulligan, Md.S. Rahaman, Removal of arsenic (III) and arsenic (V) from aqueous solutions through adsorption by Fe/Cu nanoparticles, J. Chem. Technol. Biotechnol., 93 (2018) 63–71.
[40] A. Asfaram, M. Ghaedi, S. Hajati, A. Goudarzi, E.A. Dil, Screening and optimization of highly effective ultrasound-assisted simultaneous adsorption of cationic dyes onto Mn-doped Fe_3O_4-nanoparticle-loaded activated carbon, Ultrason. Sonochem., 34 (2017) 1–12.
[41] A. Khataee, S. Saadi, B. Vahid, S.W. Joo, B.-K. Min, Sonocatalytic degradation of Acid Blue 92 using sonochemically prepared samarium doped zinc oxide nanostructures, Ultrason. Sonochem., 29 (2016) 27–38.
[42] N. Zhang, G. Xian, X. Li, P. Zhang, G. Zhang, J. Zhu, Iron based catalysts used in water treatment assisted by ultrasound: a mini review, Front. Chem., 6 (2018) 12.